Journal of Neonatal Surgery
ISSN(Online): 2226-0439
Vol. 14, Issue 6s (2025)
https://www.jneonatalsurg.com

OPEN ACCESS

Automated Kidney MRI Segmentation using connected U-Net Architecture

S. Prabhu Das[*a], B. N. Jagadeesh[b], B. Prabhakara Rao[c]

[a]Department of Electronics and Communication Engineering, JNTUK, Kakinada, INDIA.

[b]Department of Computer Science Engineering, SIET, Amalapuram, INDIA.

[c]Department of Electronics and Communication Engineering, JNTUK, Kakinada, INDIA.

Cite this paper as: S. Prabhu Das, B. N. Jagadeesh, B. Prabhakara Rao, (2025) Automated Kidney MRI Segmentation using connected U-Net Architecture. *Journal of Neonatal Surgery*, 14 (6s), 454-462.

ABSTRACT

Polycystic kidney syndrome, is a genetic disease in which the renal tubules become structurally abnormal, resulting in the outgrowth of multiple cysts and a decline in renal function. Thus, a crucial step in enhancing the quality of life for cancer patients is treatment planning. Although Magnetic Resonance Imaging (MRI) is a popular imaging method for evaluating these tumours, the volume of data it generates makes it difficult to manually segment the images in a reasonable length of time, which restricts the use of precise quantitative assessments in clinical practise. The enormous spatial and structural heterogeneity among brain tumours makes automatic segmentation a difficult task, hence effective and automatic segmentation methods are needed. UNet and its variants are one of the most advanced models for medical image segmentation, and they performed well on MRI images. So, in this paper we designed an automatic Kidney segmentation approach using Connected-UNets, which connects two UNets using additional modified skip connections. To highlight the contextual information within the encoder-decoder network design, we integrate Atrous Spatial Pyramid Pooling (ASPP) in the two conventional UNets. We also apply the proposed architecture on the Attention UNet (AUNet) and the Residual UNet (ResUNet). To evaluate the proposed model the dataset obtained from Myo clinic was considered. The experimental results give Dice Coefficient for the three architectures Connected UNets, Connected AUNets, and Connected ResUNets as 93.36%, 93.52 %, and 94.13%, and IoU score as 85.75%, 86.01%, and 87.63% respectively.

Keywords: *Magnetic Resonance Imaging, Kidney Segmentation, Deep Learning, Convolution Neural Networks, U-Net.*

1. INTRODUCTION

In the human urinary system, the kidneys play a key role in excreting waste products from blood, balancing bodily fluids and electrolytes, controlling blood pressure, and secreting hormones. As such, they are essential organs. Globally, kidney problems are a serious health concern. 1.2 million persons worldwide passed away from chronic renal disease in 2017 [1]. In 2018 saw 175,0,0 0 individuals pass away from kidney cancer, making up roughly 1.8% of all cancer-related fatalities worldwide [2]. About one in every ten live newborns is at risk of developing autosomal dominant polycystic kidney disease (ADPKD) [3]. kidney function measurement techniques should be able to predict the course of the disease, help with diagnosis and treatment, and even identify kidney lesions at an early stage. A sufficient amount of anatomical detail can be seen in high-spatial-resolution pictures produced by computed tomography (CT). As a result, it is important for diagnosing renal illness.

In addition to supporting medical radiologists or doctors in disease management, kidney segmentation in CT images can help surgeons with surgical planning and allow for the computation of the total kidney volume to assess kidney function in ADPKD [4]. On the other hand, kidney segmentation by hand requires a lot of work and time, and the outcomes are not always constant. Radiologists must invest a significant amount of time in processing the volume of CT scans [5]. Their experience has a major impact on the segmentation performance. Furthermore, some fuzzy areas may be difficult for the unaided eye to distinguish accurately. It is very expensive to manually annotate hundreds of CT images. Therefore, an automatic kidney segmentation procedure is presented in this paper which is required to satisfy clinical requirements.

The remainder of this paper is organized as follows: Section 2 reviews related works that identified the pre-processing methods and deep learning models. Then, Section 3 introduces the proposed methods, models, and pre-processing procedures to determine a kidney and tumor segmentation solution. Section 4 presents experiment to evaluate the performance metrics and validate the pre-processing procedures. Finally, discussions and conclusions are drawn in Sections 5 and 6.

2. RELATED WORK

Convolutional neural networks (CNNs) and machine learning techniques have been employed to develop numerous deep learning methods for kidney segmentation. A three-dimensional (3D) fully convolutional network consisting of a pyramid pooling module and a gradually improved feature module was proposed by Yang et al. [6]. A private dataset with an average Dice coefficient of 0.931 is used to test this network. For kidney detection and segmentation, Cuingnet et al. [7] employed the random forest algorithm and template deformation technique. A random forest classification framework was applied to dynamic contrast-enhanced images by Khalifa et al. [8]. To improve the segmentation outcome, Zhao et al. [9] suggested a multiscale supervised 3D U-Net and a CCL technique. Low-resolution labels might be accurately predicted by the multiscale supported model. Complex samples were handled using a loss-assisted, logarithmic, and exponential model. Zhao et al. used the KiTS19 local test dataset to reach a Dice coefficient of 0.969.

A triple-stage 3D U-Net with dilated convolution blocks in place of pooling operations was presented by Hou et al. [10]. The input photos for the three stages of the 3D U-Net were low-resolution, full-resolution, and cropped images. The Dice coefficient and a weighted cross-entropy were combined to create a hybrid loss function. On the KiTS19 dataset, the method's average Dice score was 0.9674. A hybrid 3D V-Net model was created by Türk et al. [11] using the ResNet++ architecture in the output layer. A V-Net-based encoder and an ET-Net-based decoder make up the model. With a Dice coefficient of 0.977, the suggested network performed better than the original V-Net. However, because it takes a lot of time and computing power, training the 3D model is difficult. There aren't many public data sets for kidney CT scans.

Numerous U-Net versions have been created to increase dice scores, and the U-Net model [12] is a well-liked design for the semantic segmentation of medical images. Isensee et al. [13] and Hou et al. [14] both employed a three-dimensional (3D) U-Net architecture in the KiTS19 Challenge. In particular, Hou et al. [14] employed multistage procedures to get accurate kidney locations and enhance tumour segmentation outcomes by employing a generic 3D U-Net, whereas Isensee et al. [13] utilised a residual 3D U-Net. A multistage approach and a residual 3D U-Net known as VB-Net, which adopted a V-Net design [15] but substituted a bottleneck structure for the traditional convolutional layers, were employed by Mu et al. [16]. Third place in the competition went to this vehicle.

Cascade U-ResNets was proposed by Xi et al. [17] to perform liver and lesion segmentation simultaneously. In order to reduce the target area and improve the precision of tumour segmentation results, cascaded approaches are frequently employed [18]. In order for the encoder to extract information, the new encoder-decoder architecture downsamples the image resolution. In order to retrieve spatial information, the decoder then upsamples the feature map [19]. An encoder-decoder model based on U-Net was utilised by Hong et al. [20]; EfficientNet replaced the encoder to achieve greater performance than the original U-Net model. Some researchers have recommended the use of transfer learning to maintain pre-trained weights from similar tasks [20,24], while others have built newer and more flexible architectures [21,23] due to the limitation of computer resources. Our main goal is to improve dice score, so we employed connected U-Net, AU-Net, and Resnet architectures for kidney segmentation in this paper.

3. METHODS

Deep learning models have recently achieved remarkable success in segmenting kidney tumors in MRI images. Recent studies involved the UNet as one of the state-of-the-art architectures and tried to modify it for a better segmentation performance. In this work, we introduced the Connected-UNets architecture for kidney tumor segmentation, which uses additional skip connection pathways to completely connect two single UNets. In addition, the network uses the ASPP technique as a transition block to get around the problem of resolution loss, especially in the case of small tumours. By revoking the first decoded characteristics and connecting them with the extra encoded inputs, the novel segmentation design increases the capacity of skip connections to rebuild the subtleties lost in the encoding pathway. The Attention UNet (AUNet) and the Residual UNet (ResUNet) are the two UNet variants on which we implemented the same design.

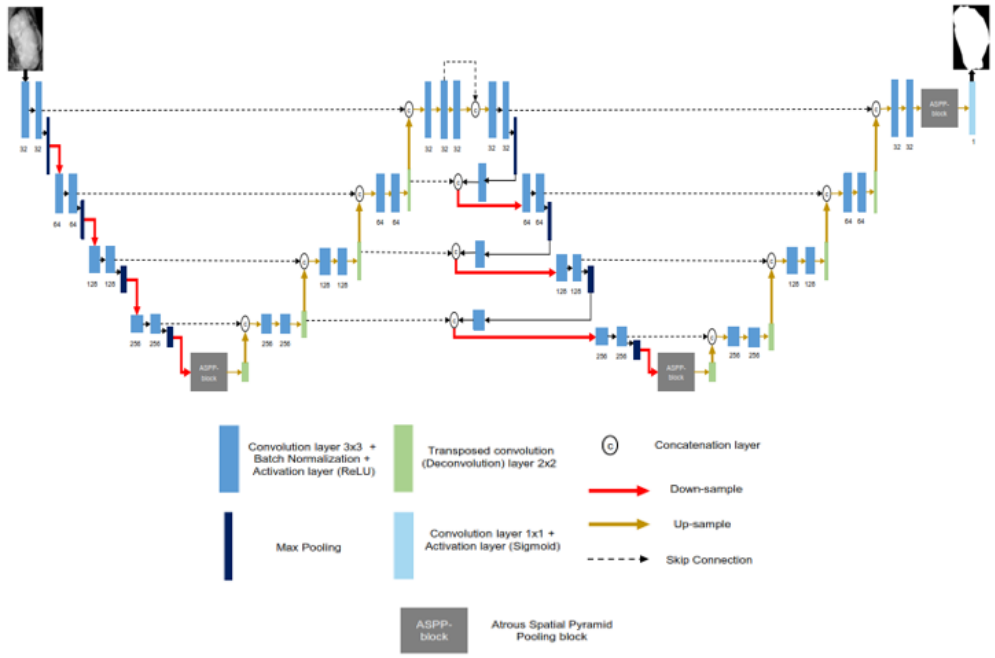

Figure 1. Connected UNet Architecture

3.1 Connected-UNets architecture

Figure 1 shows an overview of the proposed architecture, where it consists of two standard encoder and decoder blocks and two ASPP blocks for the transition between the two pathways. We suggest connecting the first decoder and the second encoder blocks with additional modified skip connections in order to reconstruct the decoded information in the first UNet before being encoded again in the second UNet. Each encoder block includes two convolution units, which consist of 3 × 3 convolutions followed by an activation ReLU (Rectified Linear Unit) and a batch normalization (BN) layer. A maximum pooling operation is then applied for the output of each encoder block before passing the information to the next encoder. Each decoder block consists of a 2 × 2 transposed convolution unit (i.e., deconvolution layer) that is concatenated with the previous encoder output, and then the result is fed into two convolution blocks, which consist of 3 × 3 convolutions followed by an activation ReLU and a BN layer.

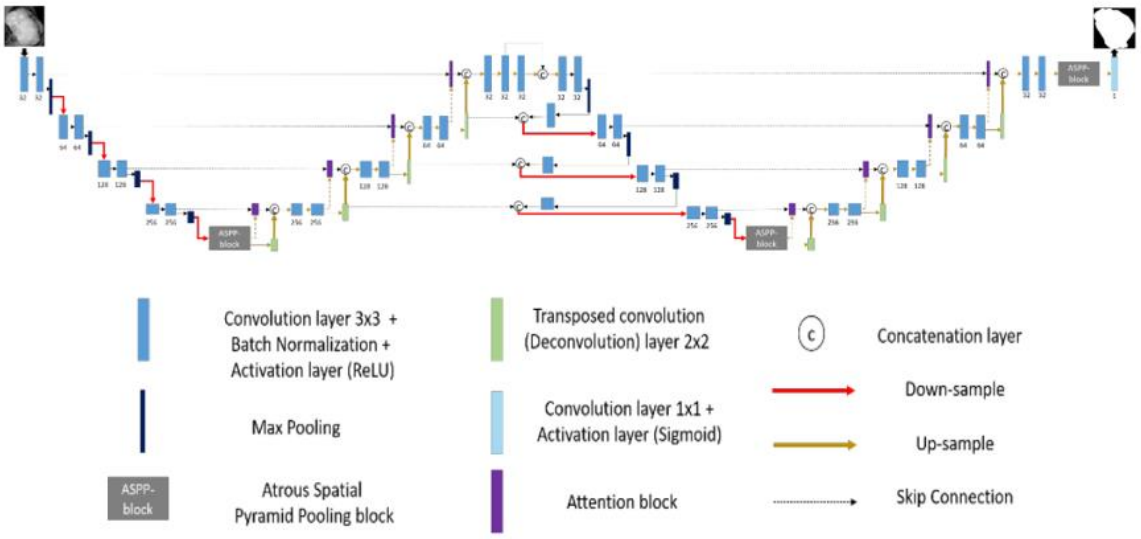

Figure 2. Connected-AUNets architecture

The transition between the down-sample and the up-sample paths is made with an ASPP block. As the name indicates, this technique uses “Atrous” (which means “holes” in French) convolution to allow having a larger receptive field in the transition

path without losing resolution. After going through the first UNet, a second UNet is attached through new skip connections that use information from the first up-sampling pathway. First, the result of the last decoder block is concatenated with the same result after being fed into a 3 × 3 convolution layer followed by an activation ReLU and a BN layer. This serves as the input of the first encoder block of the second UNet. The output of the maximum pooling operations of each three encoder blocks are fed into a 3 × 3 convolutions layers and then concatenated with the output of the last previous decoder block. The result is next down-sampled to the next encoder block. The last encoder block of the second UNet is sent into the ASPP block and the rest is similar to the first UNet, Finally, the last output is given to a 1 × 1 convolutions layer that is followed by a sigmoid activation layer to generate the predicted mask.

3.2 Connected-AUNets architecture

In addition to the proposed architecture that is applied on the standard UNet, we propose another variation by adding an attention block during the up-sampling path, called AUNet model as shown in figure 3. This integrates the attention mechanism with the skip connections between the encoder and decoder blocks. Indeed, the additional attention block should allow the network to weigh the low-level features (i.e., down-sampled information) before being concatenated with the high-level features (i.e., up-sampled information) during the skip connections. Thus, a new Connected-AUNets architecture is introduced as illustrated in Fig. 2.

3.3 Connected-Res UNets architecture

Motivated by the improvement made to the UNet architecture to be robust enough for segmenting medical images with different scales, we replace the standard convolution blocks with residual convolution blocks to become the Residual UNet (ResUNet), and consequently we proposed a Connected-ResUNets architecture as detailed in Fig. 4. Consequently, adding the residual convolution blocks should enhance the UNet architecture to reconcile the features learned at each scale of the down-sampling pathway and take full advantage of the information propagated that may cause degradation of the deep network.

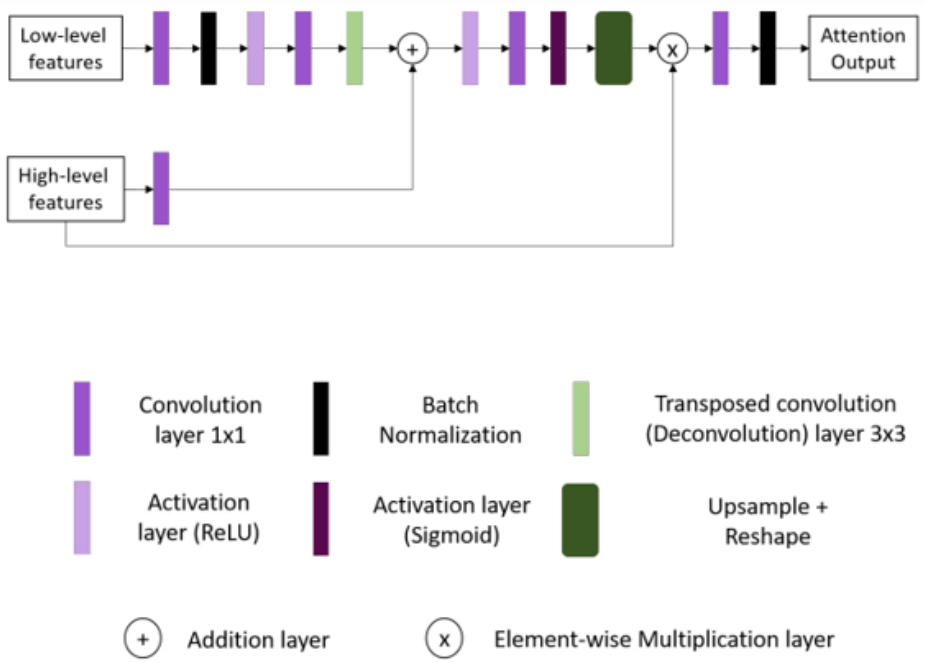

Figure 3. Attention Block

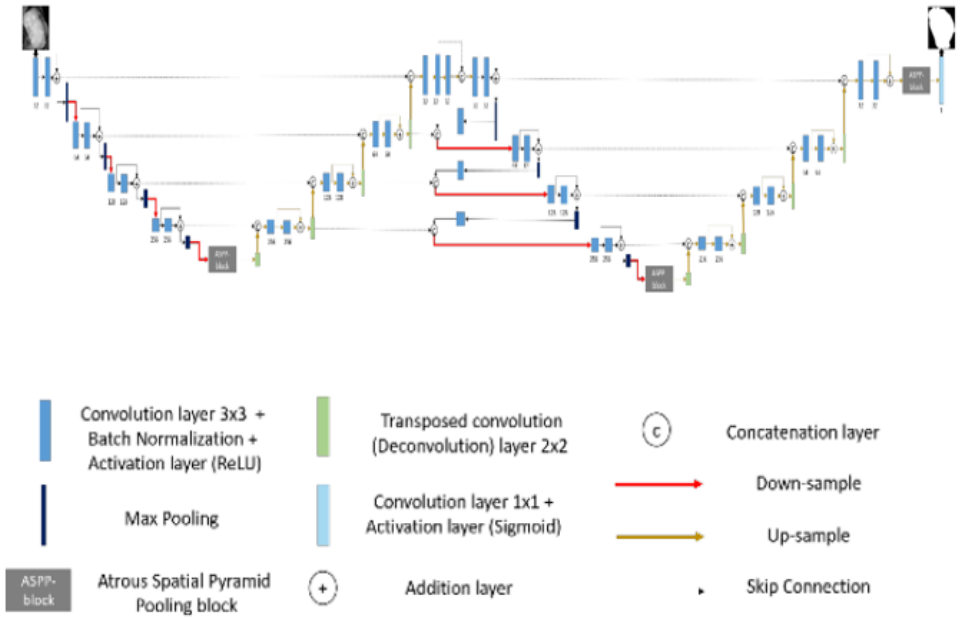

Figure 4. Connected-Res UNets architecture

3.4 Datasets

To evaluate the proposed method the dataset containing 40 MRI images is used. The dataset is obtained from Mayo Clinic [24] obtained from the 40 patients with ADPKD. The MR images were coronal single-shot fast spin-echo T2-weighted sequences that were acquired using a 1.5-T scanner (Genesis Signa, GE Healthcare) with a reconstructed matrix size of 256 × 256 × z (with z large enough to cover the full extent of the kidneys within the imaged volume). The specifications are given in the Table 1.

Table 1. Specifications

S.No	Parameter	value
1.	acquisition matrix size	256 × 128
2.	pixel size	1.5 mm
3.	slice thickness	3.0 mm
4.	slice spacing	3.0 mm
5.	TR/TE minimum	190
6.	external magnetic field (B0)	1.5 T

3.5 Evaluation Metrics

To evaluate the performance of the proposed model four metrics namely Jaccard Index, Dice coefficient, Recall and Precision are used. The dice coefficient is also called a dice similarity coefficient, it is a statistical measurement that can assess the resemblance between two different sets of data. it is used to fully assess the proposed segmentation performance within the similarity between two sets of data have been evaluated based on the dice coefficient which has been calculated using equation (1). Jaccard Index (Jac) or IoU, it is also called the Jaccard similarity coefficient, this considers as a statistic utilized in comprehending the resemblance between image sets. The measurement confirms the resemblance between finite sets of samples. In formal, it can be defined as the intersection size divided by the union size of the sets of samples. Thus, the similarity and difference among the results of ROI segmentation and the ground truth which is calculated by implementing equation (2). The recall is the ratio of the total number of true positives over the total number of ground-truth pixels (3). Precision is the ratio of the total number of true positives to the total number of predicted pixels (4).

$$\text{Dice score}(A,B) = \frac{2\times \text{Area of Intersection}(A,B)}{\text{Area of}(A) + \text{Area of}(B)} = \frac{2\times (A \cap B)}{A + B} \quad (1)$$

$$\text{IoU score}(A,B) = \frac{\text{Area of Intersection}(A,B)}{\text{Area of Union}(A,B)} = \frac{A \cap B}{A \cup B} \quad (2)$$

$$\text{Recall} = TP / TP + FN \quad (3)$$

$$\text{Precision} = TP / TP + FP \quad (4)$$

Where 'A' was the area of ROI segmentation using the proposed method, and 'B' was the ROI of the ground truth.

4. RESULTS AND DISCUSSIONS

In this section, the segmentation results of the Kidney MRI images with U-Net, Connected U-Net, AU-Net, Connected AU-Net, ResU-Net, Connected ResU-Net in terms of Dice Score and IoU scores for the datasets is presented. Clearly, from the Table 2, Connected ResU-Net gave good segmentation results.

Table 2. segmentation results for different U-Net Architectures

Proposed architectures	Dice score (%) MIAS	IoU score (%)
Standard UNet	89.21	79.5
Connected-UNets	93.36	85.75
Standard AUNet	91.35	82.59
Connected-AUNets	93.52	86.01
Standard ResUNet	92.71	84.58
Connected-ResUNets	94.13	87.63

Additionally, the area under the curve (AUC) over test sets of all datasets was used to assess the segmentation performance of our proposed Connected-UNets and its modifications against the conventional UNet, AUNet, and ResUNet. With an average AUC of 0.79 for the dataset, 0.94 for theMIAS, the proposed architectures easily beat all traditional models, as shown by Figure 5.

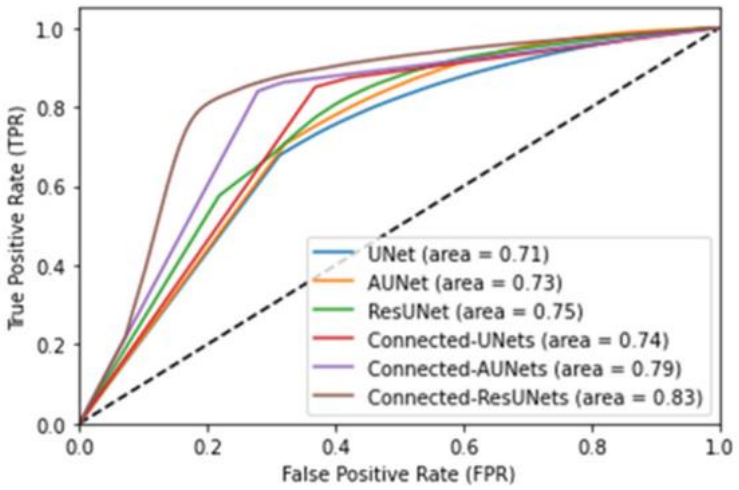

Figure 5. AUC curves for dataset

Visual aspect of the kidney segmentation approach is as shown in figure 6. Three sets of images such as 46 age man, 32 age women, and 26 age women are considered. From left to right the original image, segmented image with U-NET, Connected UNET.

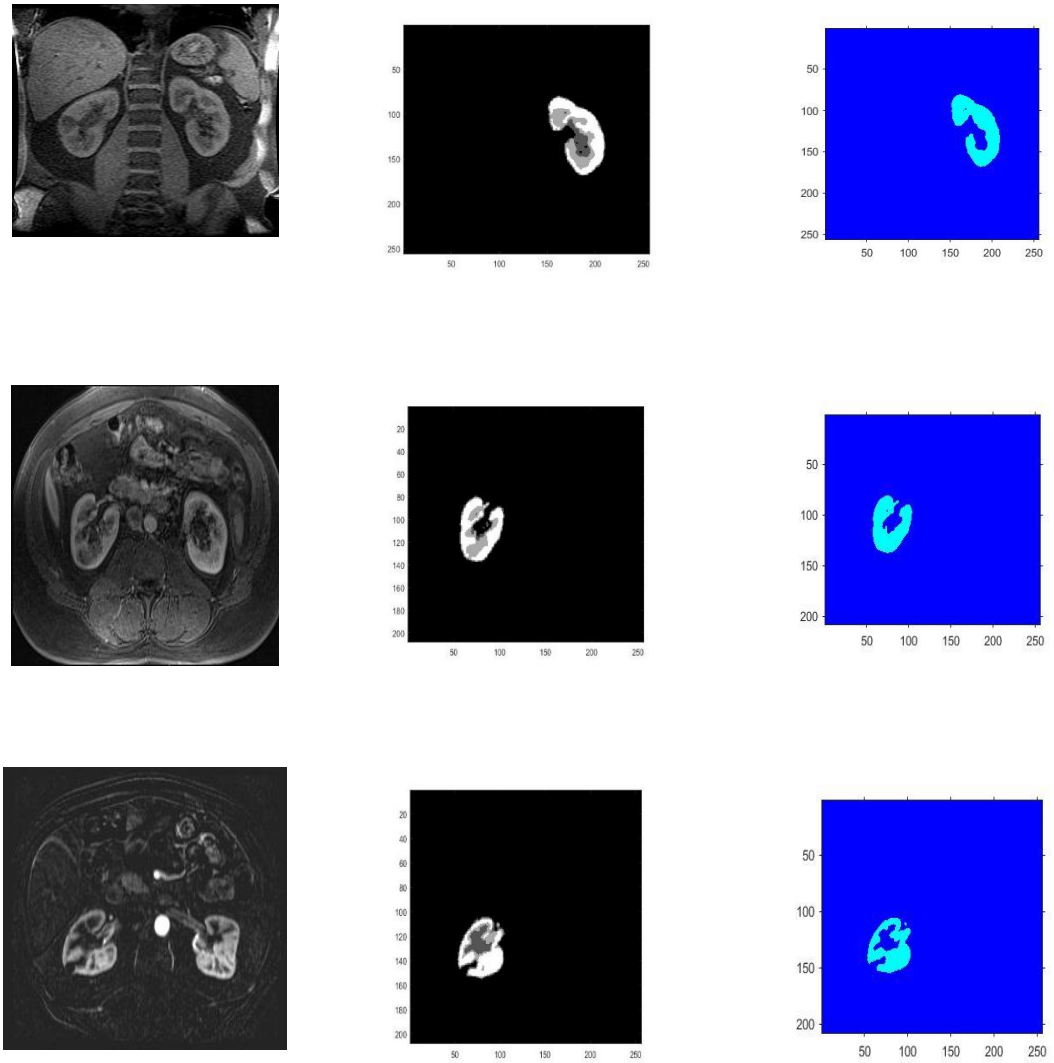

Figure 6. Visual aspect of the kidney segmentation for 3 images

Visual aspect of the kidney segmentation approach is as shown in figure. Three sets of images such as 46 age man, 32 age women, and 26 age women are considered. From left to right the original image, segmented image with U-NET, Connected UNET. Clearly, connected U-Nets gave good segmentation results.

5. CONCLUSION

In summary, we designed an automatic kidney segmentation approach using Connected-UNets, which connects two UNets using additional modified skip connections. To highlight the contextual information within the encoder-decoder network design, an Atrous Spatial Pyramid Pooling (ASPP) is integrated in the two conventional UNets. The proposed architecture is also applied on the Attention UNet (AUNet) and the Residual UNet (ResUNet). The proposed model is evaluated using myo clinic dataset with 40 MRI images. The experimental results gave superior Dice Coefficient for the three architectures Connected UNets, Connected AUNets, and Connected ResUNets. Considering the advantages of UNets, we would like to extend to more datasets.

REFERENCES

[1] B. Bikbov, C.A. Purcell, A.S. Levey, M. Smith, A. Abdoli, M. Abebe, O.M. Adebayo,M. Afarideh, S.K. Agarwal, M. Agudelo-Botero, et al., Global, regional, andnational burden of chronic kidney disease, 1990–2017: a systematic analysis for the global burden of disease study 2017, The Lancet 395 (10225) (2020) 709–733, doi: 10.1016/S0140- 6736(20)30045- 3 .

[2] Global Cancer Observatory, Cancer today, (https://gco.iarc.fr/today/home), (accessed 13 March 2021). 2021

[3] M. Levy, J. Feingold, Estimating prevalence in single-gene kidney diseases progressing to renal failure, Kidney Int. 58 (3) (20 0 0) 925–943, doi: 10.1046/j. 1523-1755.20 0 0.0 0250.x.

[4] R. Magistroni, C. Corsi, T. Martí, R. Torra, A review of the imaging techniques for measuring kidney and cyst volume in establishing autosomal dominant polycystic kidney disease progression, Am. J. Nephrol. 48 (1) (2018) 67–78, doi: 10.1159/0 0 0491022.

[5] S. Tokiwa, S. Muto, T. China, S. Horie, The relationship between renal volume and renal function in autosomal dominant polycystic kidney disease, Clin. Exp. Nephrol. 15 (4) (2011) 539–545, doi: 10.1007/s10157-011-0428-y.

[6] G. Yang, G. Li, T. Pan, Y. Kong, J. Wu, H. Shu, L. Luo, J. Dillenseger, J. Coatrieux, L. Tang, X. Zhu, Automatic segmentation of kidney and renal tumor in ct images based on 3d fully convolutional neural network with pyramid pooling module, in: 2018 24th International Conference on Pattern Recognition (ICPR), 2018, pp. 3790–3795, doi: 10.1109/ICPR.2018.8545143.

[7] R. Cuingnet, R. Prevost, D. Lesage, L.D. Cohen, B. Mory, R. Ardon, Automatic detection and segmentation of kidneys in 3d ct images using random forests, in: N. Ayache, H. Delingette, P. Golland, K. Mori (Eds.), Medical Image Computing and Computer-Assisted Intervention – MICCAI 2012, 2012, pp. 66–74, doi: 10.1007/978-3- 642- 33454- 2 _ 9.

[8] F. Khalifa, A. Soliman, A.C. Dwyer, G. Gimel'farb, A. El-Baz, A random forest-based framework for 3d kidney segmentation from dynamic contrastenhanced ct images, in: 2016 IEEE International Conference on Image Processing (ICIP), 2016, pp. 3399–3403, doi: 10.1109/ICIP.2016.7532990.

[9] W. Zhao, D. Jiang, J. Peña Queralta, T. Westerlund, Mss u-net: 3d segmentation of kidneys and tumors from ct images with a multi-scale supervised u-net, Inf. Med. Unlocked 19 (2020) 100357–100368, doi: 10.1016/j.imu.2020.100357.

[10] X. Hou, C. Xie, F. Li, J. Wang, C. Lv, G. Xie, Y. Nan, A triple-stage self-guided network for kidney tumor segmentation, in: 2020 IEEE 17th International Symposium on Biomedical Imaging (ISBI), 2020, pp. 341–344, doi: 10.1109/ISBI45749. 2020.9098609.

[11] F. Türk, M. Lüy, N. Barış¸ ç ı, Kidney and renal tumor segmentation using a hybrid v-net-based model, Mathematics 8 (10) (2020) 1772, doi: 10.3390/ math8101772.

[12] O. Ronneberger, P. Fischer, T. Brox, U-Net: convolutional networks for biomedical image segmentation, in: International Conference on Medical Image Computing and Computer-Assisted Intervention (MICCAI), 2015, pp. 234–241, doi: 10.1007/978- 3- 319- 24574- 4 _ 28 .

[13] F. Isensee, K.H. Maier-Hein, An Attempt at Beating the 3D U-Net, 2019,

[14] arXiv: 1908.02182 .

[15] X. Hou, C. Xie, F. Li, J. Wang, C. Lv, G. Xie, Y. Nan, A triple-stage self-guided network for kidney tumor segmentation, in: 2020 IEEE 17th International Symposium on Biomedical Imaging (ISBI), 2020, pp. 341–344, doi: 10.1109/ISBI45749. 2020.9098609 .

[16] F. Milletari, N. Navab, S.A. Ahmadi, V-Net: fully convolutional neural networks for volumetric medical image segmentationn, in: 2016 Fourth International Conference on 3D Vision (3DV), 2016, pp. 565–571, doi: 10.1109/3DV.2016.79 . G. Mu, Z. Lin, M. Han, G. Yao, Y. Gao, Segmentation of kidney tumor by multi-resolution VB-nets, 2019, http://results.kits-challenge.org/miccai2019/manuscripts/gr _ 6e.pdf .

[17] X.F. Xi, L. Wang, V.S. Sheng, Z. Cui, B. Fu, F. Hu, Cascade U-ResNets for simultaneous liver and lesion segmentation, IEEE Access 8 (2020) 6 8944–6 8952, doi: 10.1109/ACCESS.2020.2985671 .

[18] M.A. Hussain, G. Hamarneh, R. Garbi, Cascaded regression neural nets for kidney localization and segmentation-free volume estimation, IEEE Trans. Med. Imaging 40 (6) (2021) 1555–1567, doi: 10.1109/TMI.2021.3060465 .

[19] B. Baheti, S. Innani, S. Gajre, S. Talbar, Eff-UNet: a novel architecture for semantic segmentation in unstructured environment, in: 2020 IEEE/CVF Conference on Computer Vision and Pattern Recognition Workshops (CVPRW), 2020, pp. 1473–1481, doi: 10.1109/CVPRW50498.2020.00187 .

[20] L.T.T. Hong, N.C. Thanh, T.Q. Long, Polyp segmentation in colonoscopy images using ensembles of U-Nets with EfficientNet and asymmetric similarity loss function, in: 2020 RIVF International Conference on Computing and Communication Technologies (RIVF), 2020, pp. 1–6, doi: 10.1109/RIVF4 86 85.2020. 9140793 .

[21] Z. Zhou, M.M.R. Siddiquee, N. Tajbakhsh, J. Liang, UNet++: redesigning skip connections to exploit multiscale features in image segmentation, IEEE Trans. Med. Imaging 39 (6) (2020) 1856–1867, doi: 10.1109/TMI.2019.2959609 .

[22] X. Yan, K. Yuan, W. Zhao, S. Wang, Z. Li, S. Cui, An efficient hybrid model for kidney tumor segmentation in CT images, in: 2020 IEEE 17th International Symposium on Biomedical Imaging (ISBI), 2020, pp. 333–336, doi: 10. 1109/ISBI45749.2020.9098325 .

[23] LiverTumorSegmentationChallenge, 2017, (https://competitions.codalab.org/ competitions/17094). Accessed: 2021-01-14.

[24] European Medicines Agency (EMA). Draft qualification opinion: total kidney volume (TKV) as a prognostic biomarker for use in clinical trials evaluating patients with autosomal dominant polycystic kidney disease (ADPKD). EMA website.www.ema.europa. u/docs/en_GB/document_library/Regulatory_and_ procedural_guideline/2015/11/WC500196569.pdf. Published 2015. Accessed May 12, 2016